

## Article

# Electrophysiological Responses of *Curculio elephas* (Coleoptera: Curculionidae) to Chestnut Plant Volatiles

Eirini Anastasaki <sup>1,\*</sup> , Aikaterini Psoma <sup>1</sup>, Savvina Toufexi <sup>1</sup>, Georgios Partsinevelos <sup>1</sup> ,  
Dimitrios Papachristos <sup>1</sup> , Dimitrios Avtzis <sup>2</sup>  and Panagiotis Milonas <sup>1</sup> 

<sup>1</sup> Scientific Directorate of Entomology and Agricultural Zoology, Benaki Phytopathological Institute, 14561 Kifissia, Greece; a.psoma@bpi.gr (A.P.); s.toufexi@bpi.gr (S.T.); g.partsinevelos@bpi.gr (G.P.); d.papachristos@bpi.gr (D.P.); p.milonas@bpi.gr (P.M.)

<sup>2</sup> Forest Research Institute, Hellenic Agricultural Organization Demeter, 57006 Vassilika, Greece; dimitrios.avtzis@fri.gr

\* Correspondence: e.anastasaki@bpi.gr; Tel.: +30-210-8180372

**Abstract:** *Curculio elephas* is an oligophagous insect, attacking fruits of chestnut (*Castanea* spp.) and oak (*Quercus* spp.). It is considered one of the most important pests of European chestnut (*Castanea sativa*) in Europe and it occurs in a continuous range throughout Greece. The aim of this study was to identify the potential volatile organic compounds (VOCs) from chestnut reproductive plant tissues (catkin, nut, and bur) acting as attractants for *C. elephas* adults to be used for the development of a monitoring system integrating pest management tools. VOCs were sampled in situ during spring and autumn of 2021 and 2022 in different areas of Greece. For the collection and identification of VOCs, the dynamic-headspace technique combined with gas chromatography–mass spectrometry (GC–MS), was employed. In total, 122 compounds from these tissues were detected, with most of them being terpenes (>80%). Further analysis showed that chestnut trees release different VOCs depending on their developmental stage. Antennae of both male and female chestnut weevil adults responded to terpenes, green leaf volatiles, and methyl salicylate. Identification of semiochemicals for manipulating weevils' behavior will contribute to the development of efficient monitoring tools for the detection and management of this pest.

**Keywords:** *Curculio elephas*; chestnut; GC–MS; GC–EAD



**Citation:** Anastasaki, E.; Psoma, A.; Toufexi, S.; Partsinevelos, G.; Papachristos, D.; Avtzis, D.; Milonas, P. Electrophysiological Responses of *Curculio elephas* (Coleoptera: Curculionidae) to Chestnut Plant Volatiles. *Agriculture* **2023**, *13*, 1991. <https://doi.org/10.3390/agriculture13101991>

Academic Editor: Azucena González Coloma

Received: 15 September 2023

Revised: 10 October 2023

Accepted: 11 October 2023

Published: 13 October 2023



**Copyright:** © 2023 by the authors. Licensee MDPI, Basel, Switzerland. This article is an open access article distributed under the terms and conditions of the Creative Commons Attribution (CC BY) license (<https://creativecommons.org/licenses/by/4.0/>).

## 1. Introduction

*Curculio elephas* is an oligophagous pest, attacking chestnut (*Castanea* spp.) and oak (*Quercus* spp.) species [1,2]. It has been regarded as one of the most serious pests of European chestnut (*Castanea sativa*) in Europe and it occurs in a continuous range throughout Greece [3]. In France, adult emergence occurs between late August and October [4]; yet the exact timing of adult emergence varies greatly between countries [5]. Adult weevils emerge from the soil and move towards the nuts and mate. Females then oviposit inside the nuts [6–8]. The larvae feed on the kernel for about 2 months, making the nut unmarketable [4,9]. At the end of the larval stage, larvae exit from the fruit by chewing a hole in the pericarp and dropping to the ground, where they bury themselves in a depth ranging between 5 and 15 cm [2]. Most larvae pupate the following year, although pupation has also been observed after 2 or 3 years [8]. The damage to infested chestnuts causes an economic loss for producers [10].

Preventive management measures for *C. elephas* depend on emergence traps or visual inspection of potentially infested chestnuts. Larvae are protected within the nut and thus several applications of insecticides may be required to achieve acceptable control levels, something that can eventually result in undesirable side effects (residues, damage to natural enemies, etc.). Moreover, spray drift is also likely to occur due to the relatively large size of the trees with a negative impact on human health and biodiversity [11]. It is therefore essential to develop efficient monitoring methods and alternative control strategies.

For chestnut weevils and other plant-feeding insects in the family Curculionidae, plant odor cues are a dominant resource utilized for host selection and oviposition [12–16]. Previous studies on *C. sayi* showed that adults are attracted to and feed upon the reproductive tissues of the chestnut tree, including flowers, burs, and nuts [17]. The biology and ecology of chestnut weevil pests have been studied [18], but little is known on the chemical ecology behind this host-specific plant–insect system. Up to now, the linkage between the emitted VOCs and host plant and/or oviposition choice by *C. elephas* females has not been explored, and no sex nor aggregation pheromone has yet been identified.

In the current study, our objective was to analyze the volatile emissions at various stages of reproductive tissues (catkin, nut, and bur) in European chestnut and identify the specific volatile compounds that trigger antennal responses in *C. elephas*. Therefore, we collected and analyzed VOCs released from the headspace of the reproductive tissues of European chestnuts grown at different locations, and we examined the electrophysiological responses of *C. elephas* adults to the plant material using gas chromatography–mass spectrometry (GC–MS) and gas chromatography and electro-antennographical detection (GC–EAD). The dissimilarity in the volatile emission profiles from the tissues and the sampling locations were further analyzed by the orthogonal projections to latent structures discriminant analysis (OPLS-DA). The results of the study will provide insights for the development of a semiochemical attractant for *C. elephas*, which can be utilized as a key component of a monitoring system for the pest.

## 2. Materials and Methods

### 2.1. Insects

Dropped mature chestnuts were collected from the regional units of Chania, Crete; Arta, Epirus; and Arkadia, Peloponnese. They were transferred to the premises of Benaki Phytopathological Institute (Kifissia, Greece). Mature acorns that had dropped off the oak trees located at the premises of BPI were also collected. Chestnuts and acorns were then placed in plastic boxes covered with filter paper in an outdoor arena that allowed us to collect and count daily all mature weevil larvae that emerged spontaneously from the chestnuts and acorns during the emergence season, from mid-September to the end of December. The larvae were placed in plastic pot receptacles filled with sifted soil collected under host trees. Pots were then placed in insect rearing cages (Bugdorm, Taichung, Taiwan) and left outdoors. Adults started emerging in mid-August. We also collected adult weevils using pyramid traps [18] placed under oak trees at BPI. Newly emerged adult weevils were placed by sex, collection date, and source in insect rearing cages and were provided with 10% sugar in water [9]. Insects were kept under laboratory conditions at 25 °C temperature, 65 ± 5% relative humidity and 16 h light, 8 h dark photoperiod until used in bioassays.

### 2.2. Volatile Collection of Plant Tissues and Chemical Analysis

#### 2.2.1. Plant Tissues

Plant tissues were obtained from European chestnut trees grown in different areas in Greece during spring and autumn of 2021 and 2022. In 2021, samples were collected from chestnut trees in the area of Varnavas (V), Attika, Greece (37°14′43.7″ N 23°56′57.8″ E). In 2022, samples were taken from chestnut trees grown in the area of Ancient Feneos (F), Korinthia, Greece (37°53′34.6″ N 22°17′25.2″ E) and in the area of Kastanitsa (K), Arkadia, Greece (37°15′31.0″ N 22°38′55.9″ E). VOCs were collected four times each year (in 2021 and 2022) either in situ (1) in mid-June, from catkins clusters from chestnut in full bloom (C), (2) in mid-July, from newly fresh bur clusters (JB), and (3) in early September, in full-sized bur clusters (SB), or in the lab (4) in November from chestnuts (N).

#### 2.2.2. Chemicals

Porapak Q (80/100 mesh) was supplied from Supelco (Supelco Inc., Bellefonte, PA, USA). All solvents were MS grade and were purchased from Fisher (Fisher Scientific, Bishop, Loughborough, UK). The standard mixture of *n*-alkanes C<sub>7</sub>–C<sub>30</sub> 40 mg L<sup>−1</sup> used for

the calculation of the retention indices was purchased from Sigma-Aldrich (Steinheim, Germany). The standards used for the identification and the external calibration curves were purchased from Sigma-Aldrich (Steinheim, Germany) [butyl butanoate, (–)-*S*-citronellal, *trans*-caryophyllene, 3- $\delta$ -carene, *p*-cymene, decanal, (–)- $\beta$ -elemene, farnesene (mixture of isomers), (*Z*)-3-hexenyl acetate, (*E*)-2-hexenyl butanoate, (*Z*)-3-hexenyl butanoate, (*Z*)-3-hexenyl-2-methylbutanoate, hexyl acetate,  $\alpha$ -humulene, (–)-*S*-limonene, (+)-limonene oxide (mixture of *cis* and *trans*), 6-methyl-5-hepten-2-one,  $\beta$ -myrcene, ocimene (mixture of isomers),  $\alpha$ -phellandrene, (+)- $\alpha$ -pinene, (+)- $\beta$ -pinene, sabinene,  $\gamma$ -terpinene, (+)-valencene]; from Acros Organics (Geel, Belgium) (caryophyllene oxide, ethyl butanoate, ethyl hexanoate, ethyl octanoate, linalool, methyl hexanoate, nonanal, and octanal); from Santa Cruz Biotechnology, Inc. (Heidelberg, Germany) (butyl hexanoate, hexyl hexanoate and  $\alpha$ -terpinolene) and from TRC (Toronto, ON, Canada) [(*E*)-4,8-dimethyl-1,3,7-nonatriene and (*E,E*)-4,8,12-trimethyl-1,3,7,11-tridecatetraene]. All standards had a purity of >95%, except  $\alpha$ -phellandrene (85%) and ocimene (>90%).

### 2.2.3. Volatile Collection

VOCs were collected *in situ* or in the lab in the cases of nuts. Plant tissues and nuts were enclosed within polyethylene terephthalate (PET) oven roasting bags 12  $\mu$ m thick (SANITAS, Sarantis Group, Athens, Greece). Approximately, a branch of 60 cm long, with 3–4 catkins, as well as 3–4 bur clusters were tested. As for nuts, the same weight (250 g) was tested. VOCs collection was performed by dynamic-headspace sampling [19]. Ambient air was purified through an activated charcoal filter made with a glass tube (10 cm length  $\times$  1.5 cm i.d.) containing 0.5 g of activated charcoal (Merck, Darmstadt, Germany) tapped with glass wool (extra fine, Assistent, Berlin, Germany) and passed through the oven bag by using a Dymax 5 vacuum pump (Charles Austen Pumps Ltd., Byfleet, UK) set at 500 mL min<sup>–1</sup> by a flowmeter (Kylola, Muurame, Finland). Plant volatiles were adsorbed onto a Teflon-made trap (5 cm length  $\times$  4 mm i.d.) containing 75 mg Porapak Q, tapped with a 2 mm glass wool and 3 mm Teflon tubes on each end. Prior to use, the absorbent traps were cleaned sequentially with 1 mL methanol, diethyl ether, and *n*-pentane. The collection period *in situ* was 2 h (between 7:00 and 10:00 a.m.), while for nuts lasted 18 h. After the collection, the adsorbent traps were eluted immediately with 500  $\mu$ L of *n*-pentane. The eluates were then stored in a 2 mL vial; those of the *in situ* collection were placed in cool bags, transferred to the lab, and all vials were stored in a freezer (–20 °C) until chemical analysis. Collections of oven bags with no plants were performed. Clean absorbent traps were eluted with 500  $\mu$ L *n*-pentane as above. Background VOCs from these experiments were subtracted from treatment collections.

### 2.2.4. Gas Chromatography–Mass Spectrometry (GC–MS)

Identification of the analytes was performed in a Shimadzu Nexis GC-2030, with a QP2020 NX single quadrupole mass spectrometer (Shimadzu, Kyoto, Japan) equipped with a MEGA-5 MS capillary column (5% diphenyl/95% dimethyl polysiloxane), 30 m length, 0.25 mm i.d., and 0.25  $\mu$ m film thickness. One microliter of each plant extract was injected into the injector set at 250 °C in splitless mode. Helium was the carrier gas with a constant flow rate of 1 mL min<sup>–1</sup>. The oven temperature was maintained at 50 °C for 5 min, and increased at a rate of 3 °C min<sup>–1</sup> to 170 °C and at a rate of 20 °C min<sup>–1</sup> to the final temperature of 250 °C. The mass spectrometer was operated in electron ionization mode (EI) with ion energy of –70 eV, filament current 50  $\mu$ A, and source temperature 200 °C. Data acquisition was performed in full scan (MS) with a scanning range of 40–300 amu. We calculated the retention index (RI) of a series of *n*-alkane (C<sub>7</sub>–C<sub>30</sub>). Compounds were identified by comparing their elution order, the RI, the mass spectra with those of standards compounds, mass spectra libraries (NIST17, Wiley7), and the literature data [20,21]. The total ion chromatogram was processed by LAB solutions software (version 4) based on the retention time and mass spectrum.

Peak areas have been quantified through external standard calibration curves with standard synthetic compounds according to Anastasaki et al. [19].

### 2.3. Electrophysiological Responses

#### 2.3.1. Antenna Preparation

Both female and male adults' antenna were tested. Antennae preparation was adopted as described by Kessey [22]. The antennae were pulled from the head and were mounted on an antenna fork holder (Syntec, Buchenbach, Germany) using electroconductive gel Spectra 360 (Parker Laboratories Inc., Fairfield, NJ, USA).

#### 2.3.2. Gas Chromatography–Flame Ionization–Electroantennographic Detection (GC–FID–EAD)

Electrophysiological responses of *C. elephas* adults were tested with a Thermo Scientific TRACE 1300 Series GC chromatograph (Milan, Italy) equipped with a flame ionization detector (FID) and coupled to an electroantennographic recorder Syntec IDAC-2 (Syntec, Kirchzarten, Germany). Two  $\mu\text{L}$  of the plant extracts were injected manually in the injector set at 250 °C in the spitless mode. A TG-5MS capillary column, 30 m length, 0.25 mm i.d., and 0.25  $\mu\text{m}$  film thickness (Thermo Scientific, Waltham, MA, USA) with helium as a carrier gas at 1 mL/min was used for the volatiles' separation. The same gradient temperature program as on the VOCs' identification was also used. At the end of the column, a 3-Port SilFlow (Thermo Scientific, Milan, Italy) splits the elution with a ratio 1:1 into two 60 cm long 170  $\mu\text{m}$  i.d. deactivated tubes (Thermo Scientific, Milan, Italy). One tube leads to the FID, and the other through a heated (250 °C) transfer line (Syntec, Kirchzarten, Germany) to a glass tube. When the aliquot of the extract exits the transfer line, it is mixed with a charcoal-filtered and humidified constant airstream directed to the antenna that is controlled by a stimulus controller (CS 55, Syntec, Kirchzarten, Germany). The EAG probe with the two antennae was placed 0.5 cm from the glass tube exit. The GcEad 32 software (Syntec, Kirchzarten, Germany) was used to record the antennal and FID responses. A response was considered consistent when at least half of the antennae responded to the tested compound [23].

### 2.4. Statistical Analysis

Volatile compounds, measured as peak area and quantified using the external calibration curve, were log-transformed, scaled with the Pareto method, and processed by orthological projections to latent structures discriminant analysis (OPLS-DA) using SIMCA 18 software (Sartorius Stedim Data Analytics AB, Umeå, Sweden). VOCs' data were also subjected to hierarchical clustering (heatmap) using MetaboAnalyst v5.0 (McGill University-Xia Lab, Montreal, QC, Canada). Data were log-transformed, averaged and range scaled. The Ward-linkage clustering was used, based on the Euclidean distances. The non-parametric Kruskal–Wallis test was performed to identify differences in the quantities of the total VOCs' emissions and for each identified compound among different treatments, and Wilcoxon's test was used to test the total VOCs' emissions of burs in the two different collection periods. Both analyses were performed by SPSS version 29.0.0.0, (IBM SPSS Statistics).

## 3. Results

### 3.1. Volatile Analysis

The detected compounds in the headspace of chestnut plant tissues are shown in Table 1. The VOC profile of catkin tissues (C) and burs collected in July (JB) and September (SB) share several common compounds (Figure 1). The main class categories that have been detected were terpenes, esters, alcohols, and hydrocarbons. (*E*)- $\beta$ -caryophyllene was the only compound found in all samples from all regions. Longifolene was found in all chestnut tissues collected from the Varnavas region. (*Z*)-3-hexen-1-ol, (*Z*)-3-hexenyl acetate,  $\alpha$ -pinene, sabinene, myrcene, limonene, (*E*)- $\beta$ -ocimene, and nonanal were found in all samples of catkins and burs.



**Table 1.** Volatile compounds detected in the headspace of catkins from Varnava (CV), Feneos (CK), Kastanitsa (CK); burs collected in mid-July from Varnavas (JBV), Feneos (JBF), Kastanitsa (JBK); burs collected in early September from Varnavas (SBV), Feneos (SBF), and Kastanitsa (SBK) and from nuts collected from Varnavas (NV), Feneos (NF), and Kastanitsa (NK). The EAD-active compounds on female (F) and male (M) antennae are shown.

														Catkins			Burs				Nuts			F	M
No	RI <sub>1</sub> <sup>1</sup>	RI <sub>c</sub> <sup>2</sup>	Compound	CV	CF	CK	JBV	JBF	JBK	SBV	SBF	SBK	NV	NF	NK	EAD (n = 7)	Active (n = 5)								
1	797	798	(Z)-3-Hexenal			• <sup>3</sup>																			
2	802	798	Ethyl butanoate	•	•	•																			
3	846	841	Ethyl 2-methylbutanoate	•	•																				
4	850	849	(Z)-3-Hexen-1-ol	•	•	•	•	•	•	•	•	•				√ <sup>4</sup>	√								
5	854	852	(Z)-2-Hexen-1-ol	•																					
6	863	860	n-Hexanol	•																					
7	864	868	o-Xylene										•												
8	894	889	1-Nonene					•																	
9	900	900	n-Nonane					•																	
10	911	913	n-Amyl acetate			•																			
11	924	925	α-thujene		•	•	•	•		•															
12	932	929	α-pinene	•	•	•	•	•	•	•	•	•		•		√	√								
13	938	935	Ethyl tiglate	•																					
14	946	947	Camphene	•	•	•	•	•	•	•	•	•		•	•	√									
15	969	970	Sabinene	•	•	•	•	•	•	•	•	•	•			√	√								
16	974	978	β-pinene	•	•	•	•	•	•	•	•	•		•	•	√	√								
17	988	988	β-Myrcene	•	•	•	•	•	•	•	•	•				√	√								
18	981	988	6-Methyl-5-hepten-2-one						•			•		•											
19	995	990	2,2,4,6,6-Pentamethyl-heptane										•												
20	993	993	Butyl butyrate		•																				
21	997	998	Ethyl hexanoate	•	•	•																			
22	1000	1000	n-decane				•	•																	
23	1001	1002	2-δ-carene				•																		
24	1002	1004	α-Phellandrene					•																	
25	1001	1006	(E)-3-Hexenyl acetate	•	•	•	•	•	•																
26	1004	1008	(Z)-3-Hexenyl acetate	•	•	•	•	•	•	•	•	•				√	√								
27	1008	1010	3-δ-carene				•								•										
28	1010	1013	(E)-2-Hexenyl acetate	•	•	•	•	•	•	•															
29	1007	1014	Hexyl acetate	•	•	•	•	•	•																
30	1014	1016	α-Terpinene	•	•	•	•	•	•	•	•		•												
31	1020	1025	p-cymene	•	•	•	•	•	•	•	•		•												
32	1030	1029	Limonene	•	•	•	•	•	•	•	•	•	•	•	•										
33	1031	1030	β-phelladrene	•	•	•	•	•	•	•	•		•												
34	1026	1031	eucalyptol	•	•	•		•	•	•	•														
35	1032	1035	(Z)-β-Ocimene	•	•	•	•	•	•	•	•														
36	1037	1039	Benzyl alcohol		•																				
37	1044	1048	(E)-β-Ocimene	•	•	•	•	•	•	•	•	•				√	√								
38		1052	Alkane 1										•												
39		1055	Unknown 1							•			•												
40	1059	1059	γ-Terpinene	•	•	•	•	•	•	•	•	•	•				√								
41	1061	1062	α-Methyl Benzenemethanol	•	•	•																			
42	1059	1069	Acetophenone	•	•	•																			
43	1086	1085	α-terpinolene	•	•	•	•	•		•	•		•				√								
44	1084	1087	(E)-Linalool oxide (furanoid)	•	•	•																			
45	1092	1092	1-Undecene					•																	
46	1099	1096	α-Pinene oxide	•		•																			
47	1099	1097	Methyl benzoate	•	•																				
48	1100	1100	Undecane					•					•												
49	1095	1101	(Z)-3-Hexenyl propanoate			•		•																	
50	1101	1101	Linalool	•	•	•	•							•	•										
51	1100	1107	n-Nonanal	•	•	•	•	•	•	•	•	•		•											
52	1117	1117	(E)-DMNT	•	•	•	•	•	•	•	•			•	•										
53	1128	1128	(E)-Allo-ocimene	•	•	•	•	•		•															
54	1130	1132	(E,E)-Cosmene	•																					
55	1140	1141	neo-allo-ocimene	•	•		•																		
56	1142	1143	(Z)-3-hexenyl isobutanoate	•	•	•		•																	
57	1150	1152	Camphor											•											
58	1163	1168	p-Ethylbenzaldehyde				•					•													
59	1169	1173	Ethyl benzoate	•	•	•																			
60	1184	1184	(Z)-Cinerone	•																					
61	1184	1184	4-Terpineol		•		•	•		•			•												

Table 1. Cont.

No	RI <sub>I</sub> <sup>1</sup>	RI <sub>C</sub> <sup>2</sup>	Compound	Catkins					Burs				Nuts			F	M	
				CV	CF	CK	JBV	JBF	JBK	SBV	SBF	SBK	NV	NF	NK	EAD (n = 7)	Active (n = 5)	
62	1187	1187	(Z)-3-Hexenyl butanoate	•	•	•	•	•	•								✓	
63	1187	1192	n-dodecene		•		•	•	•	•	•							
64	1191	1193	Hexyl butanoate	•														
65	1195	1195	Methyl salicylate	•	•	•	•	•	•					•	•		✓	✓
66	1200	1199	n-Dodecane	•	•		•	•	•	•	•			•	•	•	✓	
67	1209	1209	Decanal	•		•	•	•	•	•	•		•		•			
68	1209	1211	(3E,5E)-2,6-Dimethylocta-3,5,7-trien-2-ol	•														
69	1229	1232	(Z)-3-Hexenyl 2-methyl butanoate	•	•	•	•	•	•									
70	1237	1237	(Z)-2-hexenyl isovalerate	•	•	•	•	•										
71		1247	Unknown 2				•											
72		1258	Unknown 3	•	•		•				•	•	•					
73		1267	m-Ethylacetophenone		•	•	•		•	•	•	•	•					
74	1270	1271	Ethyl salicylate	•	•	•												
75		1272	Alkane 2											•				
76	1279	1288	p-Ethylacetophenone		•		•	•	•	•	•	•	•					
77	1290	1291	n-Tridecene				•	•				•						
78	1300	1300	n-Tridecene	•			•	•				•				•		
79	1319	1324	(Z)-Hex-3-enyl	•														
80	1335	1330	(E)-2-methylbut-2-enoate	•														
81		1348	δ-Elemene	•														
82		1348	alkane 3												•			
82		1374	ester												•			
83	1374	1374	α-Copaene	•														
84	1374	1376	longicyclene											•				
85	1378	1381	(Z)-3-hexenyl hexanoate	•														
86	1388	1393	1-Tetradecene					•										
87	1400	1400	n-Tetradecane	•				•				•				•		
88	1407	1409	Longifolene	•			•			•	•			•				
89	1419	1419	(E)-β-Caryophyllene	•	•	•	•	•	•	•	•	•	•	•	•	•		
90	1419	1425	β-Cedrene	•										•				
91	1429	1437	cis-Thujopsene											•				
92	1444	1438	p-Acetylacetophenone				•											
93	1453	1450	(E)-Geranylacetone						•						•	•		
94	1452	1457	α-Humulene	•			•	•						•				
95	1458	1459	allo-Aromadendrene	•														
96	1462	1462	cis-Muurolo-4(15),5-diene	•														
97		1476	terpene											•				
98	1484	1480	Germacrene D	•	•	•	•	•			•			•			•	
99	1493	1490	α-Zingiberene	•	•	•	•			•								
100	1489	1491	β-Selinene											•				
101		1491	sesquiterpene										•					
102	1493	1493	1-Pentadecene					•										
103	1494	1495	Bicyclogermacrene	•	•													
104	1498	1497	α-Selinene											•				
105	1500	1500	Pentadecane		•	•	•	•								•		
106	1505	1504	(E,E)-α-Farnesene	•	•	•	•	•	•	•	•	•		•	•	•		
107	1505	1505	β-bisabolene				•											
108	1513	1513	γ-Cadinene	•														
109	1522	1518	δ-Cadinene	•														
110	1561	1562	(E)-Nerolidol	•														
111	1565	1574	(Z)-3-Hexenyl benzoate	•	•	•												
112	1577	1579	Spathulenol	•	•		•											
113		1597	sesquiterpene			•												
114	1582	1583	Caryophyllene oxide	•	•		•	•			•							
115	1600	1600	n-hexadecane													•		
116	1640	1634	Hinesol											•				
117		1637	terpene											•				
118	1652	1659	α-Eudesmol											•				
119	1700	1701	Heptadecane											•				
120	1800	1800	Octadecane											•				
121	1807	1807	2-Ethylhexyl salicylate				•	•										
122	1828	1830	Isopropyl myristate	•				•					•	•				

<sup>1</sup> RI<sub>I</sub>: Retention index values obtained from [20,21]. <sup>2</sup> RI<sub>C</sub>: Retention index values were calculated relative to C<sub>7–30</sub> *n*-alkanes on a column with 5% diphenyl/95% dimethyl polysiloxane stationary phase. <sup>3</sup> The dot means that the compound was detected. <sup>4</sup> “✓” indicates the EAD-active compounds on *C. elephas* antennae.

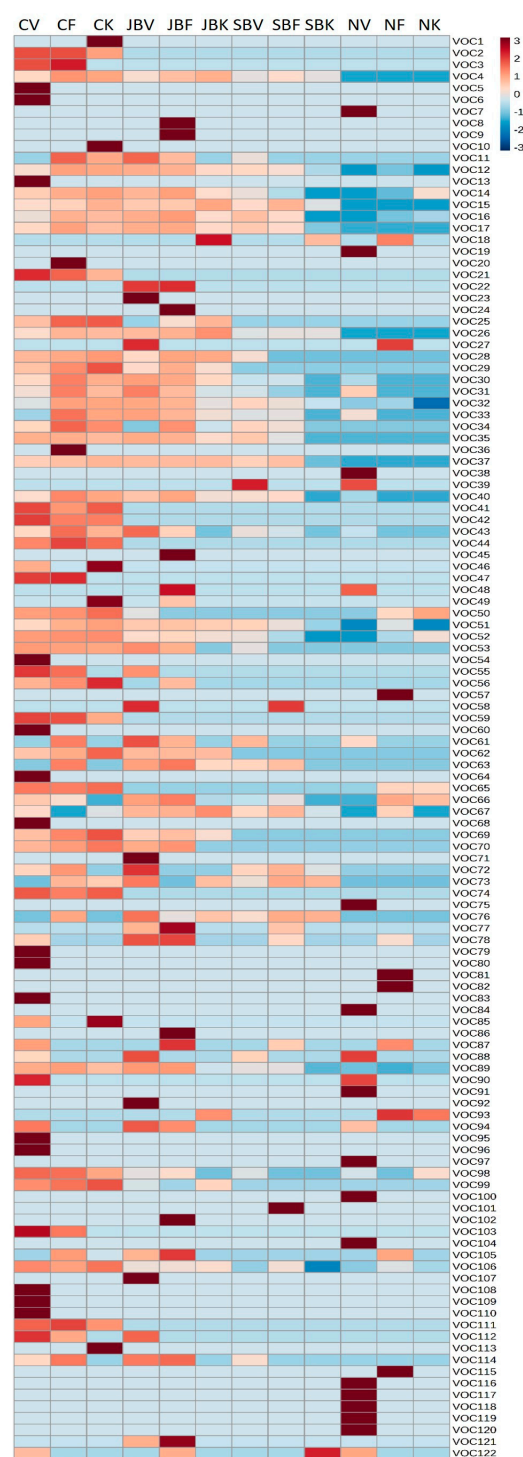


**Figure 1.** Heatmap applied on the average of volatile emissions of compounds detected in the headspace of the plant tissue of catkins from Varnava (CV)  $n = 6$ , Feneos (CF)  $n = 8$ , Kastanitsa (CK)  $n = 6$ ; burs collected in mid-July from Varnavas (JBV)  $n = 10$ , Feneos (JBF)  $n = 10$ , Kastanitsa (JBK)  $n = 5$ ; burs collected in early September from Varnavas (SBV)  $n = 7$ , Feneos (SBF)  $n = 7$ , Kastanitsa (SBK)  $n = 4$  and from nuts collected from Varnavas (NV)  $n = 3$ , Feneos (NF)  $n = 3$ , Kastanitsa (NK)  $n = 3$ . For VOCs' interpretation refer to Table 1. The red color indicates high volatile emissions, whereas blue color represents low volatile emissions.

Volatile profiles differed greatly between tree phenological stages with large fluctuations in all VOC emissions (Figure 1, Tables S1–S4). Total emissions differ significantly

between the phenological stage within each collection area ( $\chi^2 = 18.389$ ,  $df = 3$ ,  $p < 0.001$  for Varnavas;  $\chi^2 = 22.226$ ,  $df = 3$ ,  $p < 0.001$  for Feneos;  $\chi^2 = 15.789$ ,  $df = 3$ ,  $p = 0.001$  for Kastanitsa). Catkins (C) and new fresh bur clusters collected in July (JB) had significantly higher emissions compared to full-sized bur clusters collected in early September (SB) and nuts (N). Catkins (C) and burs (JB and SB) share common VOCs, that nonetheless differed in their emissions individually (Figure 1). This observation is supported by OPLS-DA models that were created in order to discriminate and classify plant tissue samples according to their developmental stage in the three regions. As shown in Figures 2–4, samples from catkins, burs, and nuts can be readily distinguished according to their VOC profile regardless of their origin. For example, plant tissues from Varnavas are dispersed but distinctly clustered in the scatter plot (Figure 2a), with burs collected during September (SBV) and nuts (SV) situated closely but remaining differentiated. The percentage of samples in the prediction set correctly classified were 100%. A similar pattern was revealed in the scatter plot of Feneos (Figure 3a), with the same two plant tissues being even closer, though the percentage of samples in the prediction set correctly classified again reached 100%. Only in the case of Kastanitsa (Figure 4a), the prediction set correctly classified decreased at 77.78%, due to the misclassification of nuts (NK) and burs (SBK). Additionally, biplots were also constructed to reveal the relationship between variables and scores.

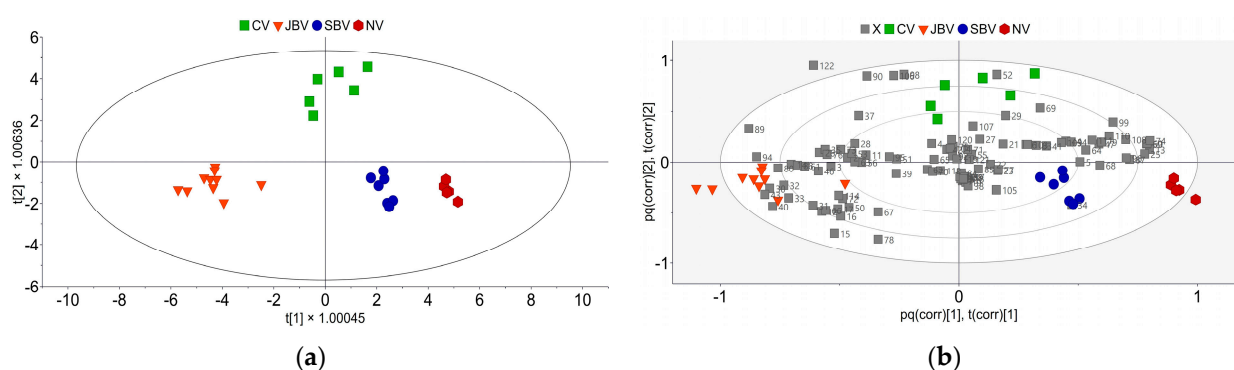


**Figure 2.** Orthogonal projection to latent structures discriminant analysis (OPLS-DA) on the volatile compounds in the headspace of plant tissues collected from Varnavas, catkins (CV), burs collected in mid-July (JBV), burs collected in early September (SBV), and nuts (NV): (a) Scatter plot; (b) Biplot. Different treatments are indicated by different shapes and colors; X dots refer to chemical variables (VOCs) with their names indicated in Table 1.

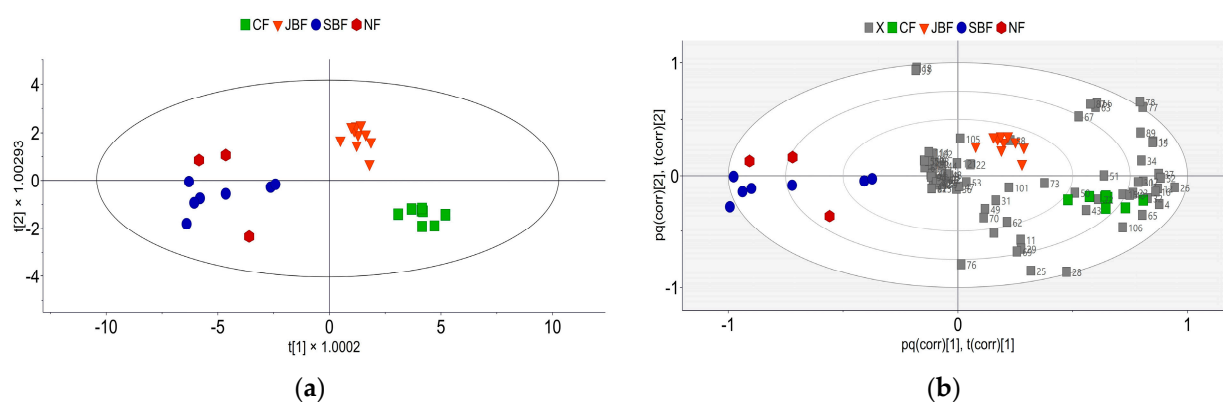


**Figure 3.** Orthogonal projection to latent structures discriminant analysis (OPLS-DA) on the volatile compounds in the headspace of plant tissues collected from Feneos, catkins (CF), burs collected in mid-July (JBF), burs collected in early September (SBF), and nuts (NF): (a) Scatter plot; (b) Biplot. Different treatments are indicated by different shapes and colors; X dots refer to chemical variables (VOCs) with their names indicated in Table 1.

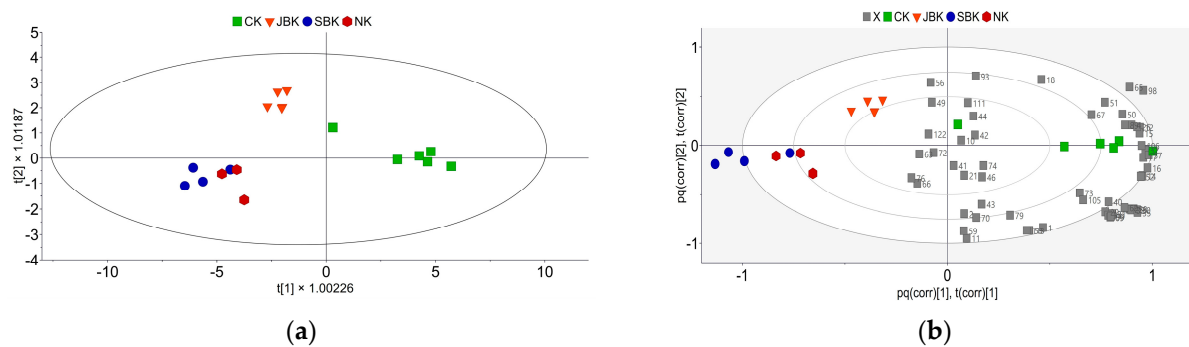


**Figure 4.** Orthogonal projection to latent structures discriminant analysis (OPLS-DA) on the volatile compounds in the headspace of plant tissues collected from Kastanitsa, catkins (CK), burs collected in mid-July (JBK), burs collected in early September (SBK), and nuts (NK): (a) Scatter plot; (b) Biplot. Different treatments are indicated by different shapes and colors; X dots refer to chemical variables (VOCs) with their names indicated in Table 1.

### 3.1.1. Catkins

In total, 72 compounds were detected in the headspace of catkin tissues collected from catkins in Varnavas (CV), 56 from catkins in Feneos (CF), and 50 from catkins in Kastanitsa (CK). Total emissions did not differ significantly between the three regions ( $\chi^2 = 0.485$ ,  $df = 2$ ,  $p = 0.785$ ), but differences were observed between the VOCs (Table S1). The major compound detected in CV and CK was *E*- $\beta$ -ocimene ( $151 \pm 47$  and  $227 \pm 44$   $\mu\text{g/h}$ , respectively), while in the headspace of CF, the two main compounds were sabinene ( $141 \pm 19$   $\mu\text{g/h}$ ) and (*E*)- $\beta$ -ocimene ( $132 \pm 30$   $\mu\text{g/h}$ ), followed by (*Z*)-3-hexenyl acetate (Table S1). Acetophenone, ethyl butanoate, ethyl hexanoate,  $\alpha$ -methyl benzenemethanol, *E*-linalool oxide, ethyl benzoate, bicyclogermacrene, and 3*Z*-hexenyl benzoate were found in all catkins' samples.

The OPLS-DA model was performed resulting in two predictive and two orthogonal components ( $R^2X = 90.4\%$ ,  $R^2Y = 96.7\%$ ,  $Q^2 = 92.3\%$ ), and showed that catkin samples from different regions can be separated according to their volatile profile (Figure 5). The percentage of samples in the prediction set correctly classified was 100%.

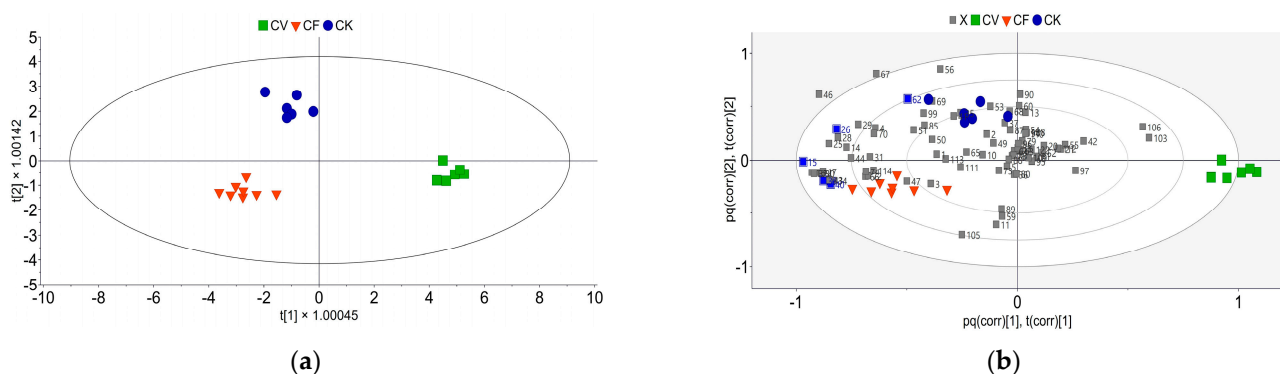


**Figure 5.** Orthogonal projection to latent structures discriminant analysis (OPLS-DA) on the volatile compounds in the headspace of catkins from Varnavas (CV), Feneos (CF), and Kastanitsa (CK): (a) Scatter plot; (b) Biplot. Different treatments are indicated by different shapes and colors; X dots refer to chemical variables (VOCs) with their names indicated in Table 1.

### 3.1.2. Burs

Burs were collected in mid-July (JB) from newly fresh bur clusters and in early September (SB) from full-sized bur clusters. (*Z*)-3-Hexen-1-ol,  $\alpha$ -pinene, sabinene, myrcene, (*Z*)-3-hexenyl acetate, limonene, (*E*)- $\beta$ -ocimene, nonanal, decanal, and (*E*)- $\beta$ -caryophyllene were the compounds detected in both collecting periods for all three regions. The headspace



of burs collected in mid-July in Varnavas (JBV) and burs collected in early September in Varnavas (SBV) were also characterized by a high amount of myrcene (Tables S2 and S3).

Newly fresh bur clusters had higher emissions compared to bur clusters collected in early September in all three regions ( $Z = -3.045$ ,  $p = 0.002$  for Varnavas;  $Z = -3.416$ ,  $p < 0.001$  for Feneos;  $Z = -2.449$ ,  $p = 0.014$  for Kastanitsa). Sabinene emissions fluctuated between 5 and 54  $\mu\text{g/h}$  in mid-July, while in early September, emissions decreased between 0.7 and 13  $\mu\text{g/h}$ . (*E*)- $\beta$ -ocimene emissions were found between 2 and 85  $\mu\text{g/h}$  in mid-July and between 0.02 and 8  $\mu\text{g/h}$  in early September. The headspace of newly fresh bur clusters of Varnavas (JBV) and Feneos (JBF) were the most abundant in total emissions and differed significantly from the one of Kastanitsa's (JBK) ( $\chi^2 = 13.846$ ,  $\text{df} = 2$ ,  $p < 0.001$ ), while the total emissions of full-sized bur (SB) clusters did not differ significantly between the three regions ( $\chi^2 = 4.514$ ,  $\text{df} = 2$ ,  $p = 0.105$ ).

The OPLS-DA models that were built for both collection periods revealed that samples can be clustered into its region (Figure 6a,c). The OPLS-DA model was performed using the samples of mid-July, resulting in two predictive and two orthogonal components ( $R^2X = 81.2\%$ ,  $R^2Y = 92.2\%$ ,  $Q^2 = 87.7\%$ ), while the one for early September burs resulting in two predictive and one orthogonal component ( $R^2X = 78.0\%$ ,  $R^2Y = 72.7\%$ ,  $Q^2 = 52.1\%$ ) revealing a clear discrimination between the three classes of samples. The percentage of samples in the prediction set of newly bur clusters correctly classified was 100%, and the one in burs collected in September was 94.44%. Additional OPLS-DA models were constructed with all samples (Figure 7a,c). It was evident that samples could also be separated according to their collection period (Figure 7c). In both cases, the corrected classification rates were 100%.

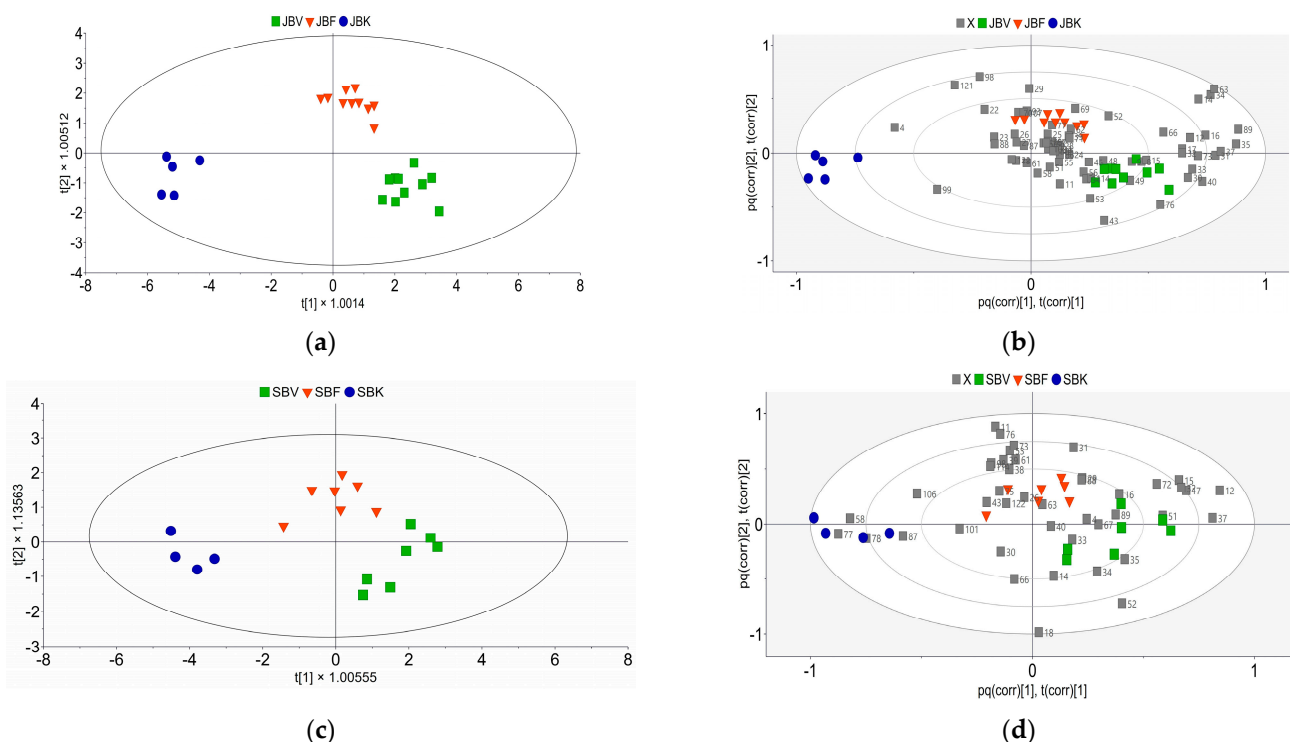


**Figure 6.** Orthogonal projection to latent structures discriminant analysis (OPLS-DA) on the volatile compounds in the headspace of bur clusters from the three regions: (a) Scatter plot for burs collected in mid-July from Varnavas (JBV), Feneos (JBF), and Kastanitsa (JBK); (b) The corresponding biplot burs collected in mid-July; (c) Scatter plot burs collected in in early September from Varnavas (SBV), Feneos (SBF), and Kastanitsa (SBK); (d) The corresponding biplot burs collected in early September. Different treatments are indicated by different shapes and colors; X dots refer to chemical variables (VOCs) with their names indicated in Table 1.

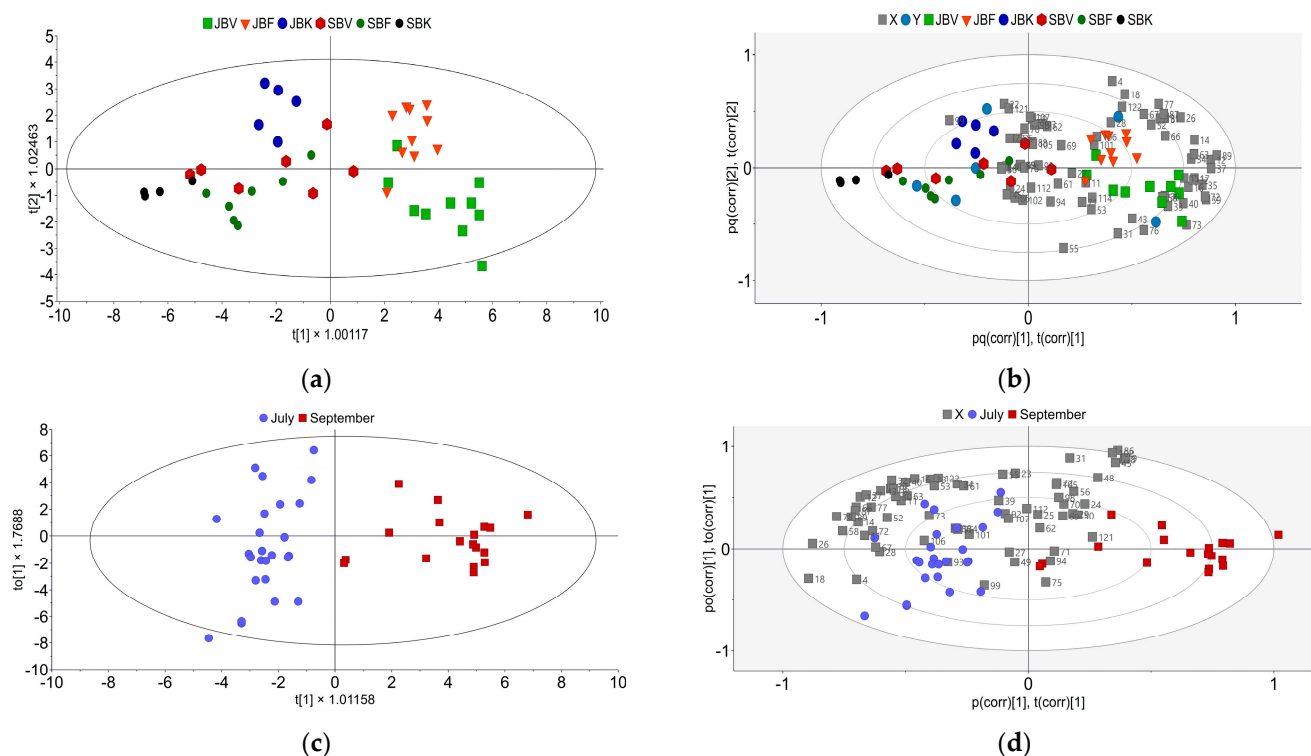


**Figure 7.** Orthogonal projection to latent structures discriminant analysis (OPLS-DA) on the volatile compounds in the headspace of bur clusters: (a) Scatter plot for all burs collected in both collection periods, mid-July (JB) and early September (SB) from Varnavas (JBV), (SBV), Feneos (JBF), (SBF), and Kastanitsa (JBK) (SBK); (b) The corresponding biplot for all burs; (c) Scatter plot burs according to their collection period July and September; (d) The corresponding biplot burs. Different treatments are indicated by different shapes and colors; X dots refer to chemical variables (VOCs) with their names indicated in Table 1.

### 3.1.3. Nuts

Nuts had considerably different VOCs compared to catkins and burs (Figure 1, Table 1). A relatively small number of VOCs were observed in the headspace of nuts. There were also qualitative variations between the three regions, however, the total emissions did not differ significantly ( $\chi^2 = 4.315$ ,  $df = 2$ ,  $p = 0.116$ ). In nut samples collected from Varnavas (NV),  $\alpha$ -eudesmol and *p*-cymene were the main compounds, followed by *o*-xylene. Most of the VOCs detected were monoterpenes, sesquiterpenes, and alkanes. The main compounds on the headspace of nuts from Feneos (NF) were limonene and linalool. Linalool was also the main compound of nuts from Kastanitsa (NK). Quantitative results showed also that only amounts of (*E,E*)- $\alpha$ -farnesene were significantly different ( $\chi^2 = 8.727$ ,  $df = 2$ ,  $p = 0.013$ ) (Table S4). However, the chemometric analysis revealed that NK and NV samples could not be differentiated (Figure 8), reaching the percentage of corrected classified samples at 66.67%.

### 3.2. GC-EAD

The chestnut plant extracts collected were further used to determine the compounds that may cause electrophysiological responses to female and male adults of *C. elephas*. We observed that the antennae of both *C. elephas* females and males responded to several compounds. The EAD-active compounds to adult female and male antennae are shown in Table 1.

The antennae of females responded to 11 EAG compounds, while the ones of males to 9 compounds (Table 1). The common compounds that stimulated an antenna response in both sexes were (*Z*)-3-hexen-1-ol,  $\alpha$ -pinene, sabinene, myrcene, (*Z*)-3-hexenyl acetate,

*E*- $\beta$ -ocimene, and methyl salicylate (Figure 9). Additionally, both sexes were electrophysiologically responding at two time points where no FID peaks were attributed. Camphene,  $\beta$ -pinene, (*Z*)-3-hexenyl butanoate, and dodecane were EAD-active for female antennae. The terpenes,  $\alpha$ -terpinolene, and  $\gamma$ -terpinene stimulated a response to male antennae.

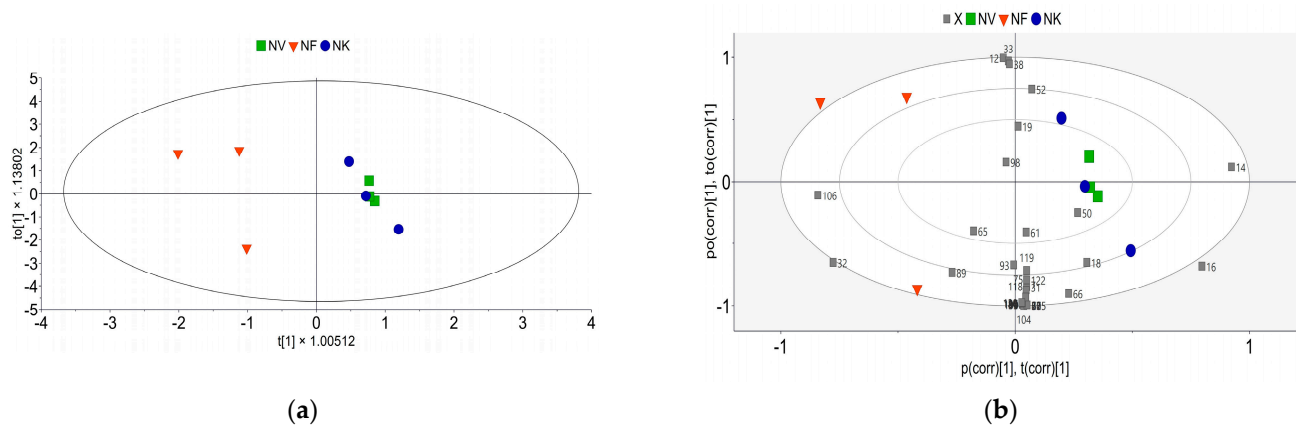


**Figure 8.** Orthogonal projection to latent structures discriminant analysis (OPLS-DA) on the volatile compounds in the headspace of nuts from Varnavas (NV), Feneos (NF), and Kastanitsa (NK): (a) Scatter plot; (b) Biplot. Different treatments are indicated by different shapes and colors; X dots refer to chemical variables (VOCs) with their names indicated in Table 1.

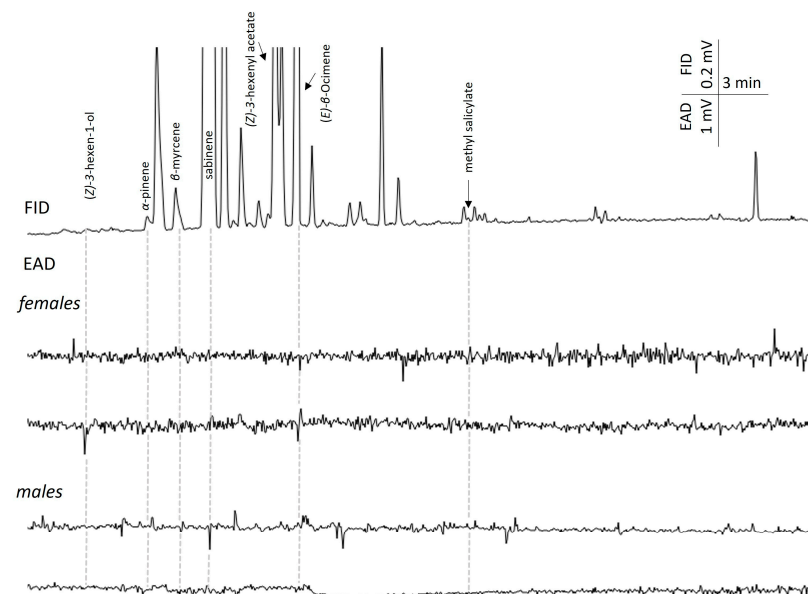


**Figure 9.** GC-EAD traces of females and males of *C. elephas* to volatiles of a bur sample collected in mid-July from Feneos.

#### 4. Discussion

Our study sheds light on the VOC profile of different tissues of *Castanea sativa* Mill. and how these specific compounds can be detected from *C. elephas* adults' antennae. Each chestnut phenological stage emitted unique volatile profiles either in blend composition (qualitative) or in relative level of emissions (quantitative) across the growing season. There were even slight variations in the volatile profiles according to the geographical origin, something that might be attributed to the cultivars planted in each region and not necessarily to different developmental conditions among regions. There is still no clear differentiation of cultivars in Greece in general [24].

Scarce literature exists on the volatile profiles of different intact plant tissues of *C. sativa* Mill. since previous studies were mostly based on cut plant tissues. For example, VOCs from sweet chestnut catkins have been analyzed, after extraction with polar and non-polar solvents [25,26], or using SPME in fresh-cut chestnut catkin samples [27]. The main compounds in the headspace of cut chestnut catkins were acetophenone, methyl salicylate, nonanal, and linalool [27], which were also in the current study, though not as the main compounds. The organic extract of flowers had a different profile with 1-phenylethanol, nonanal, benzyl alcohol, and nonanoic acid accounting for almost 80% of the extract [25]. The differences may be because volatiles in previous studies were collected in situ from the whole catkins on the branches of sweet chestnut trees, including vegetative parts, and not catkin tissues cut from the branches.

Furthermore, in the previous studies, nuts were analyzed fresh [28], dried [29,30], roasted [31], and always grided, using either SPME [28,29,31] or extraction techniques [30]. In our study, whole nuts were analyzed raw and unpeeled, and the most abundant components were terpenes and sesquiterpenes (Table S1). The VOC profile in grid dried Italian chestnut fruits [29,31] has been also characterized mainly by terpenes. On the other hand, in raw grid unpeeled chestnuts, the only terpene identified was limonene and the predominant class of VOCs was alcohol [28].

Finally, regarding burs of sweet chestnut, there is no previous study attempting to assess their VOCs. In a single related study on the Chinese chestnut, *Castanea mollissima* Blume, burs were characterized by a high amount of 4-hexenol acetate, ethyl acetate, (Z)-3-hexenol, and *n*-hexyl acetate [9]. (Z)-3-hexenol and esters were also retrieved in our study in bur clusters collected in both July and September.

Beside the VOCs profiles from different plant tissues of sweet chestnut, our study attempts for the first time to assess the EAG responses of *C. elephas* adults to sweet chestnut volatiles. Even though several compounds induced electrophysiological responses to both sexes, some of them had a rather profound impact. In particular, green leaf volatiles (GLV), (Z)-3-hexenyl acetate, and (Z)-3-hexenol have been detected by the antennae of both sexes. GLV are known to elicit significant antennal responses to other weevil species [14,16,17,32–35] and to species in other insect families [15]. They are synthesized via the hydroperoxide lyase (HPL) branch of the oxylipin pathway and can be found in all green plants while they are commonly induced after herbivory [36]. The Asian chestnut gall wasp *D. kuriphilus*, another important pest of sweet chestnut, is attracted to several GLVs, including (E)-2-hexenal, (E)-2-hexenol, hexyl acetate, and (Z)-3-hexenol emitted from chestnut branches that had been previously pruned [37].

Additionally, terpenes were also electrophysiological active compounds in the bioassays with *C. elephas* antennae. Terpenes are the largest class of secondary metabolites and occur across a wide range of plants. Their biosynthesis takes place via two pathways: the mevalonate (MVA) pathway that occurs in the cytosol of plant cells and the non-mevalonate (MEP) that occurs in the plastids [38]. They play a crucial role in direct and indirect plant defenses. Terpene compounds often serve as cues for various insect species [39] including weevils [9,40]. Antennae of other weevil species responded to a wide range of terpenes [16,33–35]. Terpenes like limonene and  $\alpha$ -pinene have also been found as constituents in the headspace extracts of the conspecific female of raspberry weevils [40].

Finally, methyl salicylate (MeSA) also induced responses in both sexes. This benzenoid compound is known to trigger significant EAG responses on other weevil species [16,34]. Moreover, weevils have been shown to be attracted to this compound in behavioral assays [32]. MeSA is a widely distributed plant volatile [38], found also in the host plant of other weevils [16,41,42]. It is also an herbivore-induced plant volatile (HIPV) after herbivory by different weevils such as the strawberry blossom weevils [43].

In our GC-EAD experiments, several compounds were found to be electrophysiological active for both sexes. Olfactory cues are usually used to orientate toward a specific host plant within a plant patch [15]. Insects are guided in their effort to locate feeding hosts and oviposition sites by a variety of VOCs produced by plants [44]. Behavioral bioassays

and antennal electrophysiological studies have both shown that weevils can detect and orientate to host plant volatiles [9,16,17,41].

## 5. Conclusions

This study provides the first electroantennographic responses of *C. elephas* to volatiles emitted from sweet chestnut plant tissues. Among others, GLV and terpenes as well as MeSA have been reported to play a role in plant–insect interactions of other weevils. Further studies including bioassays and field assays are scheduled to better elucidate the role of specific compounds either as individuals or in blends that influence host plant selection and oviposition. Such an understanding of insect behavior is helpful for developing effective management strategies of *C. elephas* on chestnut trees.

**Supplementary Materials:** The following supporting information can be downloaded at: <https://www.mdpi.com/article/10.3390/agriculture13101991/s1>, Table S1: Volatile emissions of compounds detected in the headspace of catkins collected from Varnavas (CV), Fenos (CF), and Kastanitsa (CK), expressed in  $\mu\text{g h}^{-1} \pm \text{SE}$ ; Table S2: Volatile emissions of compounds detected in the headspace of newly fresh burs collected in mid-July from Varnavas (JBV), Fenos (JBF), and Kastanitsa (JBK), expressed in  $\mu\text{g h}^{-1} \pm \text{SE}$ ; Table S3: Volatile emissions of compounds detected in the headspace of full-sized bur clusters collected in early September from Varnavas (SBV), Fenos (SBF), and Kastanitsa (SBK), expressed in  $\mu\text{g h}^{-1} \pm \text{SE}$ ; Table S4: Volatile emissions of compounds detected in the headspace of nuts collected from Varnavas (NV), Fenos (NF), and Kastanitsa (NK), expressed in  $\mu\text{g h}^{-1} \pm \text{SE}$ .

**Author Contributions:** Conceptualization, E.A., D.P. and P.M.; methodology, E.A., D.A, D.P. and P.M.; software, E.A. and P.M.; validation, E.A. and P.M.; formal analysis, E.A., A.P., S.T. and G.P.; investigation, E.A., A.P., S.T., G.P. and D.P.; resources, E.A., D.P. and P.M.; data curation, E.A., A.P., D.A., D.P. and P.M.; writing—original draft preparation, E.A.; writing—review and editing, E.A., D.P, D.A. and P.M.; visualization, E.A. and A.P.; supervision, E.A, D.P. and P.M.; project administration, E.A.; funding acquisition, E.A. All authors have read and agreed to the published version of the manuscript.

**Funding:** The research project was supported by the Hellenic Foundation for Research and Innovation (H.F.R.I.) under the “2nd Call for H.F.R.I. Research Projects to support Post-Doctoral Researchers” (Project Number: 0215).

**Institutional Review Board Statement:** Not applicable.

**Data Availability Statement:** Most of the data generated or analyzed during this study are included in this published article and its Supplementary Materials. All other datasets generated during and/or analyzed during the current study are available from the corresponding author upon request.

**Acknowledgments:** We would like to thank all the farmers and growers for providing us with the area and the necessary supplies for the collection of VOCs.

**Conflicts of Interest:** The authors declare no conflict of interest. The funders had no role in the design of the study; in the collection, analyses, or interpretation of data; in the writing of the manuscript; or in the decision to publish the results.

## References

1. Bonal, R.; Munoz, A. Seed growth suppression constrains the growth of seed parasites: Premature acorn abscission reduces *Curculio elephas* larval size. *Environ. Entomol.* **2008**, *33*, 31–36. [CrossRef]
2. Paparatti, A.; Sperantza, B. Biological control of chestnut weevil (*Curculio elephas* Gyll. Coleoptera, Curculionidae) with the entomopathogen fungus *Beauveria bassiana* (Balsam) Vuill. (Deuteromycotina, Hyphomycetes). *Acta Hort.* **1999**, *494*, 459–464. [CrossRef]
3. Avtzis, D.N.; Perlerou, C.; Diamandis, S. Geographic distribution of chestnut feeding insects in Greece. *J. Pest Sci.* **2013**, *86*, 185–191. [CrossRef]
4. Menu, F. Strategies of emergence in the chestnut weevil *Curculio elephas* (Coleoptera: Curculionidae). *Oecologia* **1993**, *96*, 383–390. [CrossRef] [PubMed]
5. Venette, R.C.; Davis, E.E.; Heisler, H.; Larson, M. Mini Risk Assessment Chestnut Weevil, *Curculio elephas* (Gyllenhal) (Coleoptera: Curculionidae), USDA-APHIS CAPS Pest Risk Assessment. 2003. Available online: <https://download.ceris.purdue.edu/file/336> (accessed on 20 April 2023).



6. Debouzie, D.; Heizmann, A.; Desouhant, E.; Menu, F. Interference at several temporal and spatial scales between two chestnut insects. *Oecologia* **1996**, *108*, 151–158. [CrossRef] [PubMed]
7. Desouhant, E.; Debouzie, D.; Ploye, H.; Menu, F. Clutch size manipulations in the chestnut weevil, *Curculio elephas*: Fitness of oviposition strategies. *Oecologia* **2000**, *122*, 493–499. [CrossRef]
8. Soula, B.; Menu, F. Variability in diapause duration in the chestnut weevil: Mixed ESS, genetic polymorphism or bet-hedging? *Oikos* **2003**, *100*, 574–580. [CrossRef]
9. Keeseey, I.W.; Barrett, B.A.; Lin, C.-H.; Lerch, R.N. Electroantennographic responses of the small chestnut weevil *Curculio sayi* (Coleoptera: Curculionidae) to volatile organic compounds identified from chestnut reproductive plant tissue. *Environ. Entomol.* **2012**, *4*, 933–940. [CrossRef]
10. Alma, A.; Quacchia, A. Chestnut pests in Chestnut (*Castanea sativa*): A Multipurpose European Tree. In Proceedings of the Workshop Proceedings, Bruxelles, Belgium, 30 September–1 October 2010.
11. García-García, C.R.; Parrón, T.; Requena, M.; Alarcón, R.; Tsatsakis, A.M.; Herdández, A.F. Occupational pesticide exposure and adverse health effects at the clinical, hematological and biochemical level. *Life Sci.* **2016**, *145*, 274–283. [CrossRef] [PubMed]
12. Eller, F.J.; Bartelt, R.J.; Shasha, B.S.; Schuster, D.J.; Riley, D.G.; Stansly, P.A.; Mueller, T.F.; Shuler, K.D.; Hohnson, B.; Davis, J.H.; et al. Aggregation pheromone for the pepper weevil, *Anthonomus eugenii* cano (Coleoptera: Curculionidae): Identification and field activity. *J. Chem. Ecol.* **1994**, *20*, 1537–1555. [CrossRef]
13. Desouhant, E. Selection of fruits for oviposition by the chestnut weevil, *Curculio elephas*. *Entomol. Exp. Appl.* **1998**, *86*, 71–78. [CrossRef]
14. Van Tol, R.W.H.M.; Visser, J.H. Olfactory antennal responses of the vine weevil *Otiorhynchus sulcatus* to plant volatiles. *Entomol. Exp. Appl.* **2002**, *102*, 49–64. [CrossRef]
15. Bruce, T.J.A.; Wadhams, L.J.; Woodcock, C.M. Insect host location: A volatile situation. *Trends Plant Sci.* **2005**, *10*, 269–274. [CrossRef] [PubMed]
16. Szendrei, Z.; Malo, E.; Stelinski, L.; Rodriguez-Saona, C. Response of cranberry weevil (Coleoptera: Curculionidae) to host plant volatiles. *Environ. Entomol.* **2009**, *38*, 861–869. [CrossRef]
17. Keeseey, I.W.; Barrett, B.A. Behavioral and Electroantennographic Responses of the Lesser Chestnut Weevil, *Curculio sayi* (Coleoptera: Curculionidae), to Odors Emanating from Different Chestnut Plant Tissues. *J. Kans. Entomol. Soc.* **2012**, *85*, 145–154. [CrossRef]
18. Filgueiras, C.C.; Willet, D.S. Phenology and Monitoring of the Lesser Chestnut Weevil. *Insects* **2022**, *13*, 713. [CrossRef] [PubMed]
19. Anastasaki, E.; Drizou, F.; Milonas, P.G. Electrophysiological and oviposition responses of *Tuta absoluta* females to herbivore-induced volatiles in tomato plants. *J. Chem. Ecol.* **2018**, *44*, 288–298. [CrossRef]
20. Adams, R.P. *Identification of Essential Oil Components by Gas-Chromatography/Mass Spectrometry*, 4th ed.; Allured Business Media: Carol Stream, IL, USA, 2007.
21. NIST Standard Reference Data. Available online: <http://webbook.nist.gov/chemistry/name-ser.html> (accessed on 23 January 2023).
22. Keeseey, I.W. The Chemical Ecology of the Lesser Chestnut Weevil: Behavioral and Electrophysiological Responses of *Curculio sayi* (Coleoptera: Curculionidae) to Host-Plant Volatile Organic Compounds. Ph.D. Dissertation, University of Missouri, Columbia, MO, USA, May 2011.
23. Pinto-Zevallos, D.M.; Strapasson, P.; Zarbin, P.H.G. Herbivore-induced volatile organic compounds emitted by maize: Electrophysiological responses in *Spodoptera frugiperda* females. *Phytochem. Lett.* **2016**, *16*, 70–74. [CrossRef]
24. El Chami, M.A.; Tourvas, N.; Kazakis, P.; Aravanopoulos, F.A. Genetic characterization of chestnut cultivars in Crete. *Forests* **2021**, *12*, 1659. [CrossRef]
25. Allisandrakis, E.; Tarantilis, P.A.; Pappas, C.; Harizanis, P.C. Investigation of organic extractives from unifloral chestnut (*Castanea sativa* L.) and eucalyptus (*Eucalyptus globulus* Labill.) honeys and flowers to identification of botanical marker compounds. *LWT-Food Sci. Technol.* **2011**, *44*, 1042–1051. [CrossRef]
26. Machado, A.M.; Antunes, M.; Miguel, M.G.; Vilas-Boas, M.; Figueiredo, A.C. Volatile Profile of Portuguese Monofloral Honeys: Significance in Botanical Origin Determination. *Molecules* **2021**, *26*, 4970. [CrossRef] [PubMed]
27. Yang, Y.; Battesti, M.-J.; Djabou, N.; Muselli, A.; Paolini, J.; Tomi, P.; Costa, J. Melissopalynological origin determination and volatile composition analysis of Corsican “chestnut grove” honeys. *Food Chem.* **2012**, *132*, 2144–2154. [CrossRef]
28. Mujić, I.; Zivković, J.; Savić, V.; Alibabić, V.; Staver, M.; Jug, T.; Franić, M.; Damijanić, K. Analysis of volatile compounds in chestnut using solid-phase microextraction coupled with GC-MS. *Acta Hort.* **2018**, *1220*, 203–208. [CrossRef]
29. Cirlini, M.; Dall’Asta, C.; Silvanini, A.; Beghè, D.; Fabbri, A.; Galaverna, G.; Ganini, T. Volatile fingerprinting of chestnut flours from traditional Emilia Romagna (Italy) cultivars. *Food Chem.* **2012**, *134*, 662–668. [CrossRef]
30. Moure, A.; Cone, E.; Falqué, E.; Domínguez, H.; Parajó, J.C. Production of nutraceuticals from chestnut burs by hydrolytic treatment. *Food Res. Int.* **2014**, *65*, 359–366. [CrossRef]
31. Krist, S.; Unterweger, H.; Bandion, F.; Buchbauer, G. Volatile compound analysis of SPME headspace and extract samples from roasted Italian chestnuts (*Castanea sativa* Mill.) using GC-MS. *Eur. Food Res. Technol.* **2004**, *219*, 470–473. [CrossRef]
32. Barlet, E.; Blight, M.M.; Plane, P.; Willimas, I.H. The responses of the cabbage seed weevil *Ceutorhynchus assimilis* to volatile compounds from oilseed rape in a linear track olfactometer. *Entomol. Exp. Appl.* **1997**, *85*, 257–262. [CrossRef]

33. Pawlowski, S.P.; Sweeney, J.D.; Hillier, N.K. Electrophysiological Responses of the Beech Leaf-Mining Weevil, *Orchestes fagi*, to Seasonally-Variant Volatile Organic Compounds Emitted by American Beech, *Fagus grandifolia*. *J. Chem. Ecol.* **2020**, *46*, 935–946. [\[CrossRef\]](#)
34. Toshova, T.B.; Velchev, D.I.; Subchev, M.A.; Toth, M.; Vuts, J.; Picjett, J.A.; Dewhirst, S.Y. Electrophysiological responses and field attraction of the grey corn weevil, *Tanymecus (Episomecus) dilaticollis* Gyllenhal (Coleoptera: Curculionidae) to synthetic plant volatiles. *Chemoecology* **2010**, *20*, 199–206. [\[CrossRef\]](#)
35. Wee, S.-L.; El-Sayes, A.M.; Gibb, A.R.; Mitchell, V.; Suckling, D.M. Behavioural and electrophysiological responses of *Pantomorus cervinus* (Boheman) (Coleoptera: Curculionidae) to host plant volatiles. *Aust. J. Entomol.* **2008**, *47*, 24–31. [\[CrossRef\]](#)
36. Scala, A.; Allmann, S.; Mirabella, R.; Haring, M.A.; Schuurink, R.C. Green leaf volatiles: A plant's multifunctional weapon against herbivores and pathogens. *Int. J. Mol. Sci.* **2013**, *14*, 17781–17811. [\[CrossRef\]](#) [\[PubMed\]](#)
37. Germinara, G.; De Cristofaro, A.; Rotundo, G. Chemical cues for host location by chestnut gall wasp, *Dryocosmus kuriphilus*. *J. Chem. Ecol.* **2011**, *37*, 49–56. [\[CrossRef\]](#)
38. Kant, M.; Bleeker, P.M.; Van Wijk, M.; Schhrink, R.C.; Haring, M. Plant Volatiles in Defence. In *Advances in Botanical Research*; van Loon, L.C., Ed.; Academic Press: London, UK, 2009; Volume 51, pp. 613–666. [\[CrossRef\]](#)
39. NinKuu, V.; Zhang, L.; Yan, J.; Fu, Z.; Yang, T.; Zeng, H. Biochemistry of Terpene and Recent Advances in Plant Protection. *Int. J. Mol. Sci.* **2021**, *22*, 5710. [\[CrossRef\]](#) [\[PubMed\]](#)
40. Mutis, A.; Parra, L.; Monosalva, L.; Palma, R.; Cnadia, O.; Lizama, M.; Pardo, F.; Perich, F.; Quiro, A. Electroantennographic and Behavioral Responses of Adults of Raspberry Weevil *Aegorhinus superciliosus* (Coleoptera: Curculionidae) to Odors Released from Conspecific Females. *Environ. Entomol.* **2010**, *39*, 1276–1282. [\[CrossRef\]](#) [\[PubMed\]](#)
41. Mozuraitis, R.; Hall, D.; Trandem, N.; Ralle, B.; Tunstrom, K.; Sigsgaard, L.; Baroffio, C.; Fountain, M.; Cross, J.; Wibe, A.; et al. Composition of Strawberry Floral Volatiles and their Effects on Behavior of Strawberry Blossom Weevil, *Anthonomus rubi*. *J. Chem. Ecol.* **2020**, *46*, 1069–1081. [\[CrossRef\]](#)
42. Roberts, J.M.; Kundun, J.; Rowley, C.; Hall, D.R.; Douglas, P.; Pope, T.W. Electrophysiological and Behavioral Responses of Vine Weevil, *Otiorhynchus sulcatus* (Coleoptera: Curculionidae), Adults to Host Plant Odors. *J. Chem. Ecol.* **2019**, *45*, 858–868. [\[CrossRef\]](#)
43. Bichão, H.; Borg-Karlson, A.-K.; Araújo, J.; Mustaparta, H. Five Types of Olfactory Receptor Neurons in the Strawberry Blossom Weevil *Anthonomus rubi*: Selective Responses to Inducible Host-plant Volatiles. *Chem. Senses* **2005**, *30*, 153–170. [\[CrossRef\]](#)
44. Bruce, T.J.; Pickett, J.A. Perception of plant volatile blends by herbivorous insects-finding the right mix. *Phytochemistry* **2011**, *72*, 1605–1611. [\[CrossRef\]](#)

**Disclaimer/Publisher's Note:** The statements, opinions and data contained in all publications are solely those of the individual author(s) and contributor(s) and not of MDPI and/or the editor(s). MDPI and/or the editor(s) disclaim responsibility for any injury to people or property resulting from any ideas, methods, instructions or products referred to in the content.